this facility is the order of 0.2%). The results for model B indicate separation occurring at the shoulder and attendant higher drag levels. As expected, the drag coefficients of models B and C are quite close. Transition seems to occur in the separated shear layer and there is no apparent evidence of large scale vortex shedding.

The grooved body results are quite encouraging. The drag, for the higher Reynolds numbers, is reduced by the order of 40% and the visualization indicates the separated shear layer closure angle has moved approximately halfway toward the body. The model was tested with the grooves rotated 45 deg in the azimuthal direction from their position shown in Fig. 1. The obvious question concerning these grooved body data is "what mechanism is responsible for the drag reduction?" The original intent was that the grooves should serve simply as large scale (and continuous) longitudinal vortex generators. Extrapolation of diffuser experience with conventional vortex generators (which are usually contained within the boundary layer and of limited streamwise extent) indicated that the present 30 deg afterbody closure required a treatment considerably stronger than they could provide. A possible contributor to the present favorable results could be disruption of the shear layer instability waves ("coherent structure") by groove induced azimuthal flow variations.[7-9] Further research is required to elucidate the physical basis for the present results and optimize the effect.

References

[1] "Vehicle Aerodynamics: The Next Fuel Economy Frontier," *Automotive Engineering*, Vol. 86, July 1978, pp. 19-24.

[2] Hefner, J. N. and Bushnell, D. M., "An Overview of Concepts for Aircraft Drag Reduction," AGARD Rept. 654, 1977, pp. 1-1 - 1-30.

[3] Mair, W. A., "Drag-Reducing Techniques for Axi-Symmetric Bluff Bodies," *Aerodynamic Drag Mechanisms of Bluff Bodies and Road Vehicles*, Plenum Press, New York, 1978, pp. 161-187.

[4] Chang, P. K., *Control of Flow Separation*, Hemisphere Publishing Corp., McGraw-Hill Book Co., New York, 1976.

[5] Hefner, J. N. and Weinstein, L. M., "Re-Examination of Compliant Wall Experiments with Air with Water Substrates," *Journal of Spacecraft and Rockets*, Vol. 13, Aug. 1976, pp. 502-503.

[6] Sykes, D. M., "Blockage Corrections for Large Bluff Bodies in Wind Tunnels," *Advances in Road Vehicle Aerodynamics 1973*, edited by H. S. Stephens, BHRA Fluid Engineering, pp. 311-322.

[7] Kuethe, A. M., "Effect of Streamwise Vortices on Wake Properties Associated with Sound Generation," *Journal of Aircraft*, Vol. 9, Oct. 1972, pp. 715-719.

[8] Pannu, S. S. and Johannesen, N. H., "The Structure of Jets from Notched Nozzles," *Journal of Fluid Mechanics*, Vol. 74, Pt. 3, 1976, pp. 515-528.

[9] Bradbury, L.J.S. and Khadem, A. H., "The Distortion of a Jet by Tabs," *Journal of Fluid Mechanics*, Vol. 70, Pt. 4, 1975, pp. 801-813.

AIAA 81-4096

Stress Intensity Factors in a Biaxial Stress Field

A.F. Liu*

Northrop Corporation, Hawthorne, Calif.

IT has been discussed [1,2] that lateral tension or compression stresses would not affect the elastic stress intensity factors for a central straight crack in a plate. However, if a crack (or cracks) comes out of a circular hole in a plate, compressive loading parallel to the crack can cause tensile mode 1 stress intensity factors. On the other hand, tensile stresses parallel to the crack reduce the stress concentrations at the hole and thus reduce the crack tip stress intensity factor. Bowie's solutions[3] have provided stress intensity factors for a single crack (or cracks) emanating from the edge of a circular hole, in an infinitely wide plate, under uniaxial and the one-to-one biaxial loading conditions. For any other biaxial load ratios (either tension combined with tension or tension combined with compression), stress intensity factors can be developed by using superpositions of the uniaxial and biaxial solutions of Bowie as illustrated in Fig. 1. Following this superposition logic, stress intensity for any biaxial loading combinations can be expressed as:

$$K=[(\sigma_y-\sigma_x)B_0+\sigma_x B_1]\sqrt{\pi a} \tag{1}$$

where B_0 is the Bowie factor for uniaxial loading and B_1 is the Bowie factor for one-to-one biaxial loading; a is the crack length on either side of the hole; σ_y is the far-field gross area stress perpendicular to the crack (always in tension), and σ_x is the far-field gross area stress parallel to the crack (either in tension or compression). Let $B=\sigma_x/\sigma_y$, Eq. (1) can be written as,

$$K=\sigma_y\sqrt{\pi a}[(1-B)B_0+B\cdot B_1] \tag{2}$$

and the sign for B may be either (+) or(−).

If the hole is inside a finite width plate, the plate dimensions influence the stress concentration at the edge of the hole and thereby vary the stress intensity factor. Furthermore, finite width dimension also increases the crack tip stress intensity as if the hole was never there. Modifications to Eq. (2) have been reported in the literature (see Refs. 4 and 5 for $B=0$). For engineering purposes, Eq. (2) can be written as,

$$K=\sigma_y\sqrt{\pi a}[(1-B)B_0+B\cdot B_1]\cdot F \tag{3}$$

where F is a geometric factor accounting for the boundary effect of the specimen (e.g., width).

In a previous work of the author[6] the validity of using the compounded geometric factor was examined. The cases studied were double cracks at a hole in a specimen subjected to remote uniaxial cyclic loading. Constant amplitude crack growth rate data were obtained from specimens (made of 2024-T851 aluminum) that contained various hole radius to width ratios and a wide range of crack length-to-hole radius ratios. These data points were reduced to da/dN vs ΔK format using Eq. (3), and then compared to the material baseline da/dN curves developed from center cracked specimens of which the K-solution was known. Good correlations had been obtained.

In this investigation, eight cruciform specimens of the 7075-T7351 aluminum alloy had been tested under biaxial cyclic stresses. The geometry and dimensions of the cruciform specimens were the same as those reported in Ref. 2 but contained a circular hole of 6.35 mm, or 19.05 mm, in

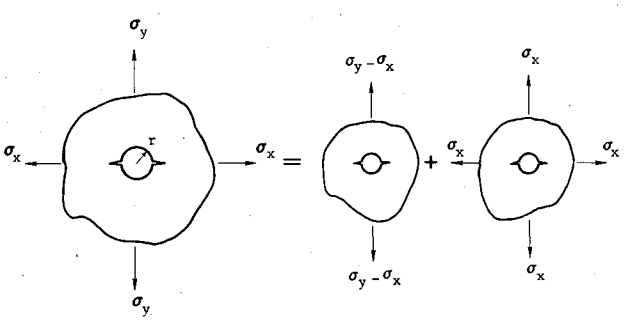

Fig. 1 Evaluation of Bowie's factor for biaxial loading.

Received Sept. 2, 1980.

*Senior Technical Specialist, Structures Life Assurance Research, Aircraft Division.

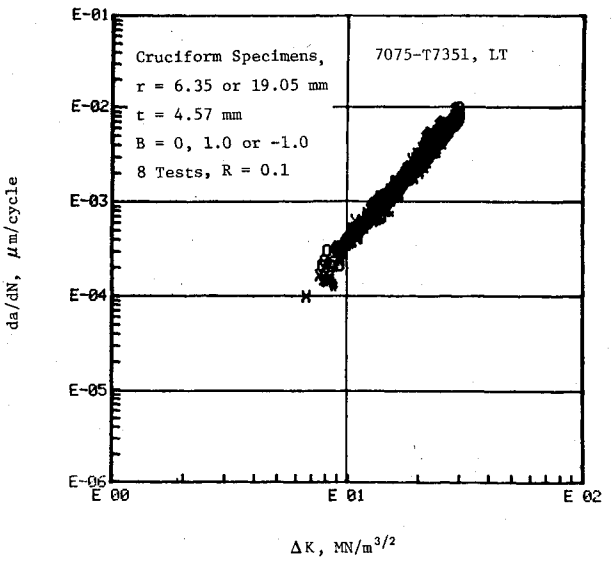

Fig. 2 Cyclic crack growth behavior for cracks at a hole.

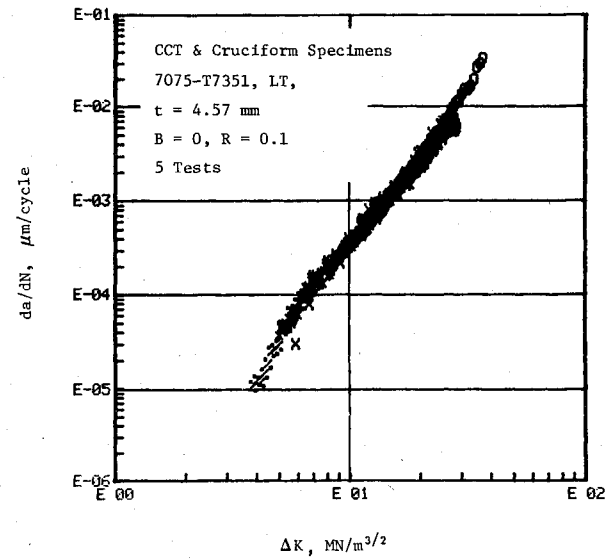

Fig. 3 Cyclic crack growth behavior of center cracked specimen.

diameter. Each specimen was cyclically precracked from a crack starter (a very small saw cut approximately 1.0 mm in length) at both sides of the hole. The stress amplitude was 82.68 MPa and 8.268 MPa for σ_y with B being either 0, +1, or −1. A crack growth history for each test was recorded. The K value for each data point was computed using the superposition technique of Eq. (3). According to Ref. 2, F was equal to unity for the cruciform specimen. All da/dN vs ΔK data points, for all eight tests at three different biaxial stress ratios, are presented in Fig. 2. A group of data points representing the baseline crack growth rate behavior of the same material (i.e., developed from specimens without a hole) is presented in Fig. 3. It is seen that the crack growth rate behavior in all seven cases (a big hole or a small hole in either one of the three biaxial loading conditions, and a baseline condition, i.e., $\sigma_x = 0$, no hole) are the same. Therefore the result of this comparison has indicated that stress intensity factors for cracks at a hole can be accurately computed by using Eq. (3).

In conclusion, it has been verified by experiments that lateral stresses parallel to the crack may or may not affect the crack tip stress intensity factor depending upon specimen geometry and crack morphology. As stated earlier, wherever there is no geometric complexity, e.g., a straight crack in a semi-infinite sheet, the K values will be the same for all the cases, i.e., with and without σ_x. Otherwise, e.g., cracks at the edge of a hole, the K-factor for a given crack will change from one biaxial ratio to another biaxial ratio. However, the crack growth rate at a given ΔK level will be the same for all the cases as long as the K value for each case is properly determined.

References

[1] Paris, P.C. and Sih, G.C., "Stress Analysis of Cracks," *Fracture Toughness Testing and its Applications,* ASTM STP 381, 1965, pp. 30-83.

[2] Liu, A.F., Allison, J.E., Dittmer, D.F. and Yamane, J.R., "Effect of Biaxial Stresses on Crack Growth," *Fracture Mechanics,* ASTM STP 677, edited by C.W. Smith, ASTM, New York, 1979, pp. 5-22.

[3] Bowie, O.L., "Analysis of an Infinite Plate Containing Radial Cracks Originating at the Boundary of an Internal Circular Hole," *Journal of Mathematics and Physics,* Vol. 35, 1956, pp. 60-71.

[4] Newman, J.C. Jr., "An Improved Method of Collocation for the Stress Analysis of Cracked Plates with Various Shaped Boundaries," NASA TN D-6376, Aug. 1971.

[5] Tada, H. Paris, P.C. and Irwin, G.R., *The Stress Analysis of Cracks Handbook,* Del Research Corporation, Hellertown, Pa., 1973.

[6] Liu, A.F., "Behavior of Cracks at a Hole," *Proceedings of the Second International Conference on Mechanical Behavior of Materials,* American Society of Metals, 1976, pp. 601-605.

AIAA 81-4097

Finite Elements for Generalized Plane Strain

M.P. Rossow*
Southern Illinois University at Edwardsville
Edwardsville, Ill.

Introduction

A SURVEY of the available textbooks on finite elements leads to the surprising observation that most authors omit even a passing reference to generalized plane strain analysis of a long, linearly elastic cylinder for which the axial force is specified. Apparently the only exception is Gallagher,[1] who proposes that the axial strain be treated as an unknown and be calculated, just like the nodal variables for the mesh, by solving the assembled stiffness equations.

Gallagher's approach is direct, clear, and theoretically elegant, but in some practical situations it has two drawbacks. First, because the axial strain directly influences the stress state in *every* element in the mesh, the stiffness matrix is not banded (the axial strain unknown appears in every equation of the assembled system). Because the stiffness matrix, even if not banded, is still sparse, this objection can be met to some extent by using an efficient equation solver (e.g., a frontal solver), which avoids unnecessary operation with zeroes. Nevertheless, the suspicion remains that there should be a way to formulate the problem so that this source of computational inefficiency is avoided altogether.

The second practical drawback to treating the axial strain as an additional unknown (like an additional nodal variable) is that implementing this approach in an existing computer program requires many conceptually trivial, but in practice, time-consuming and error-prone coding changes. The presence of "one more" variable means that indexing arrays

Received Sept. 25, 1980.

*Associate Professor, Dept. of Engineering and Technology.